Abnormal photovoltaic effects in ferroelectric ($BiFeO_3$)

Marin Alexe
University of Warwick , Physics Department,
CV8 4AL Coventry, UK

Photovoltaic effect in BFO single crystals

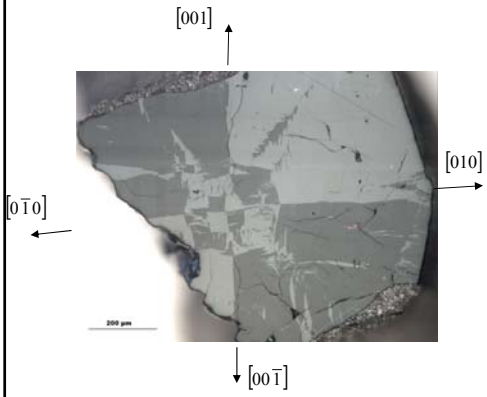

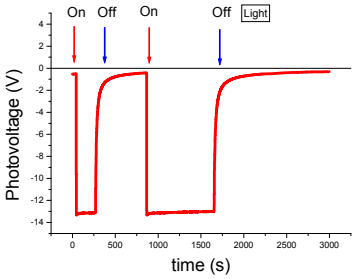

Photovoltage measured 80 mW
(λ=405 nm, $h\nu$=3.05 eV)

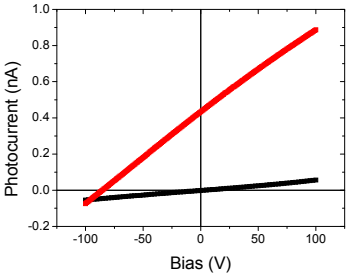

Thin film vs single crystal

Open circuit voltage – single crystal bulk

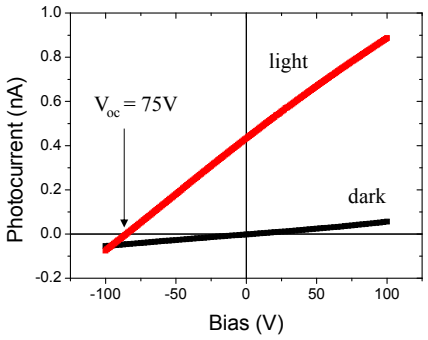

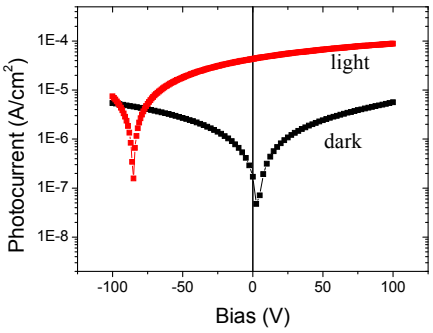

Thin film vs single crystal

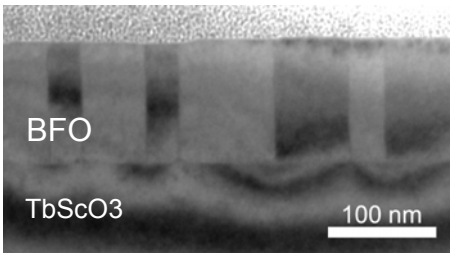

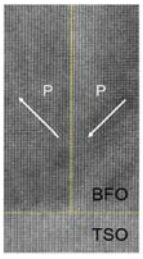

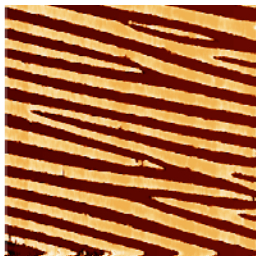

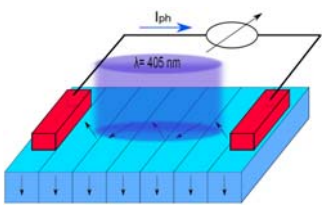

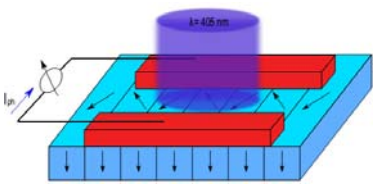

Thin film vs single crystal

Parallel

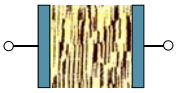

Open circuit voltage – Thin film

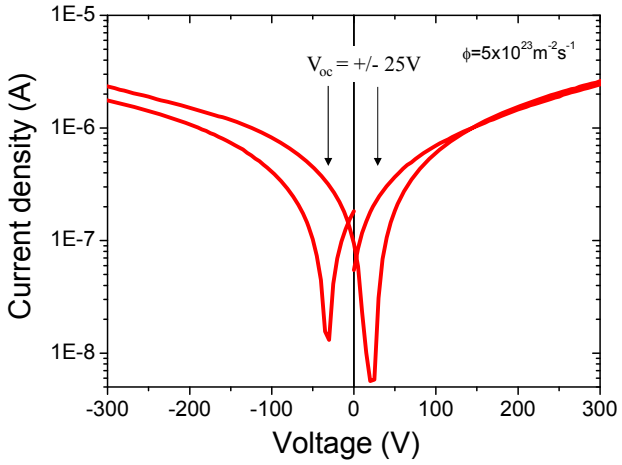

- Origins of the abnormal PV effect

Photoelectric effect

Photoconductive effect

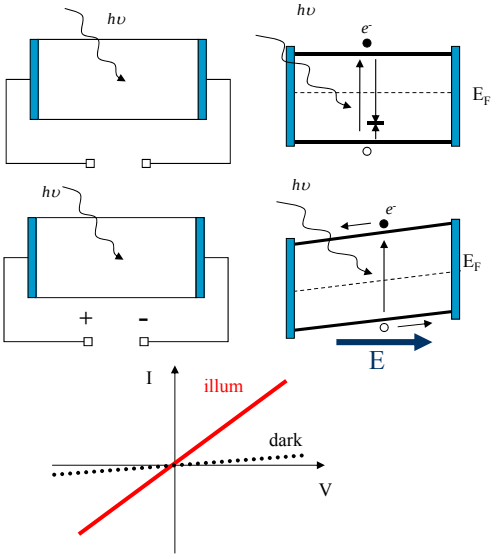

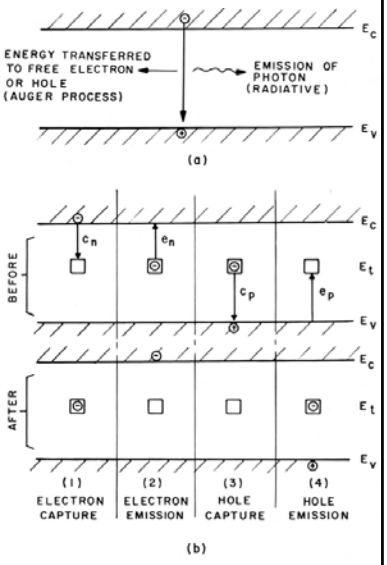

S.M. Sze, Physics of Semiconductor Devices, Wiley 1981

Photovoltaic effect

p-n junctions

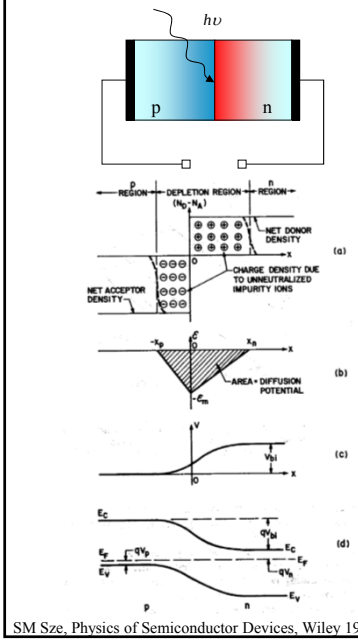

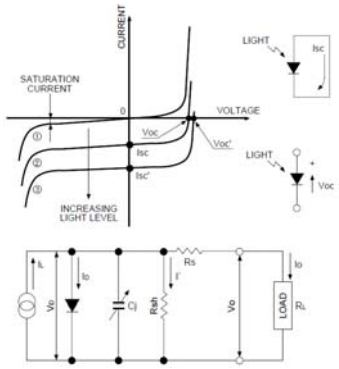

$$I_O = I_L - I_D - I' = I_L - I_S\left(exp\ \frac{eV_D}{kT} - 1\right) - I' \ .....$$

$$V_{OC} = \frac{kT}{e}\ ln\left(\frac{I_L - I'}{I_S} + 1\right)$$

I_L – photogenerated current
I_D – diode current
I' – shunt current
I_S – reverse saturation current

SM Sze, Physics of Semiconductor Devices, Wiley 1981

Microscopic origins of APV

THE ORIGIN OF THE PHOTO-EMF IN FERROELECTRIC AND NON-FERROELECTRIC MATERIALS

W. RUPPEL, R. VON BALTZ and P. WÜRFEL

Department of Physics, University of Karlsruhe, D-7500 Karlsruhe, West Germany

(Received June 3, 1981)

$f_{ph}(\mathbf{r}, \mathbf{k}) = f_{eq}[\epsilon_k - \eta(\mathbf{r})] + \delta f(\mathbf{r}, \mathbf{k})$ Carrier distribution function under photo-excitation

$f_{eq}(\epsilon_k - \eta) = \{1 + \exp[(\epsilon_k - \eta)/k_B T]\}^{-1}$ Carrier distribution function at equilibrium, Symmetric in k-space, can not generate current

$$\delta f(\mathbf{r}, \mathbf{k}) = \tau \cdot G_{opt}(\mathbf{r}, \mathbf{k}) + \frac{\partial f_{eq}(\epsilon_k - \eta)}{\partial(\epsilon_k - \eta)} \cdot v_k \cdot \nabla_r \eta(\mathbf{r})$$

lifetime; Generation rate; internal field

ϵ_k – energy; η = quasi-Fermi level

9

Microscopic origins of APV

1. $\nabla\eta(r) \neq 0$ Classical case: gradient in Fermi level (chemical potential)
2. $G(+k) \neq G(-k)$ APV case: Generation rate asymmetric in k-space

$$\delta f^{as}(k) = \frac{1}{2}[G(+k) - G(-k)]\tau = G^{as}\tau$$

$$\mathbf{j}_{PG} = \sum_k - e\tau v_k G^{as} = -e\mathbf{l}(G^+ - G^-)$$ Photo-galvanic current

Example of asymmetric potential in pyroelectric crystal

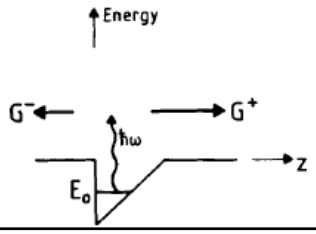

10

Abnormal photovoltaic effect

- The abnormal photovoltaic effect or photogalvanic (photo-ferroelectric) effect

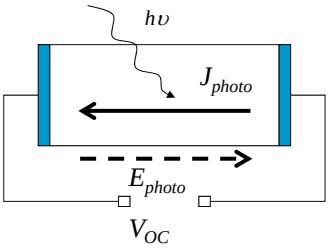

- In steady-state the photocurrent should be zero
- An internal field E_{photo} builds up to cancel the non-equilibrium carriers

Condition: Δn>> n0
(photo generated carrier density much higher than the thermally activated)

Anomalous Photovoltaic Effect

$$J^* = J + (\sigma_d + \sigma_{ph})E$$

- J* is the transitional photocurrent density,
- J is the photovoltaic current density,
- σ_d and σ_{ph} are the dark and photoconductivities,
- E is the electric field formed due to the charging with photovoltaic current

$$V_{oc} = \frac{J}{\sigma_d + \sigma_{ph}} l$$

- V_{oc} is the open circuit voltage
- l is the distance between electrodes

Fridkin, V. M., Photoferroelectrics,
Springer-Verlag Berlin Heidelberg New York, 1979

12

Thin film vs single crystal

Parallel

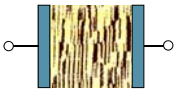

Open circuit voltage – Thin film

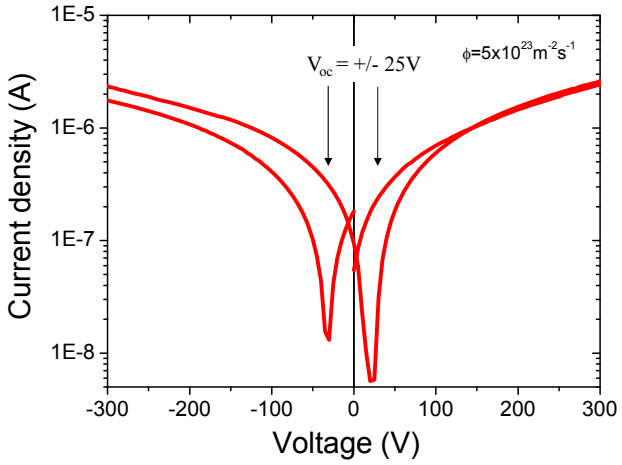

APV effect

- The abnormal photovoltaic effect in BFO is solely due to photogalvanic (photo-ferroelectric) effect or bulk PVE
- The BPV photocurrent is tensorial in nature
- It depends solely by the crystalline structure

Time-resolved photoelectric force microscopy for high resolution mapping of recombination centers

Photoelectric force microscopy

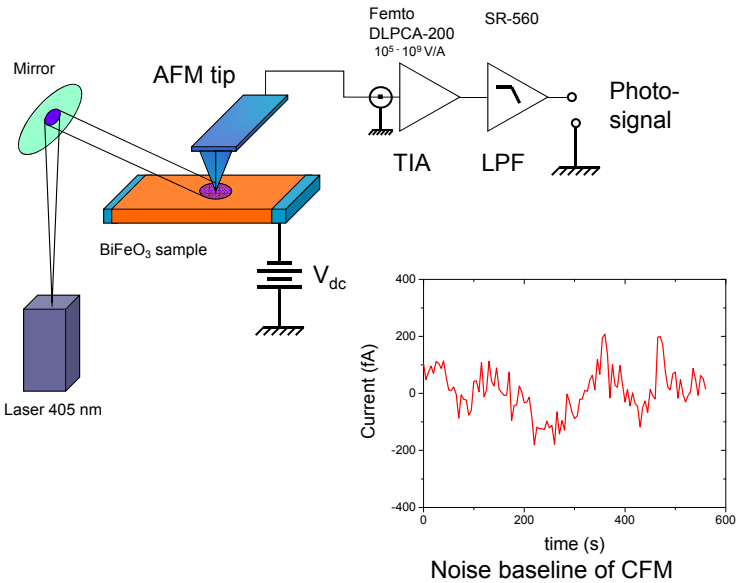

Noise baseline of CFM

Ph-AFM scan across the BFO domains

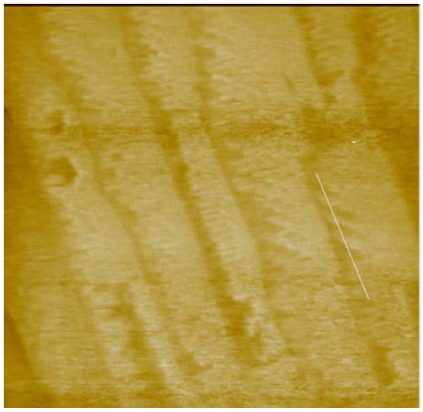

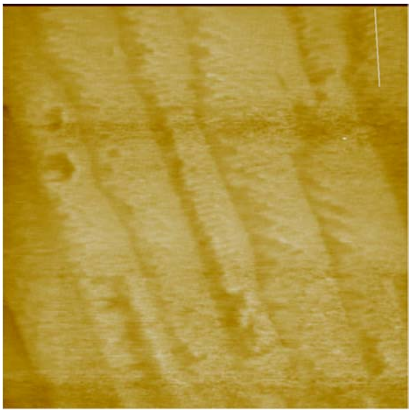

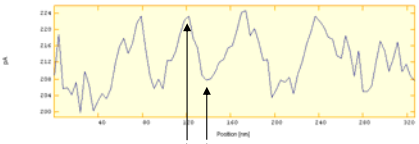

250 nm

Resolution ~ 20 nm ; tip contact diameter

z-PFM

Topography Amplitude Phase PhAFM

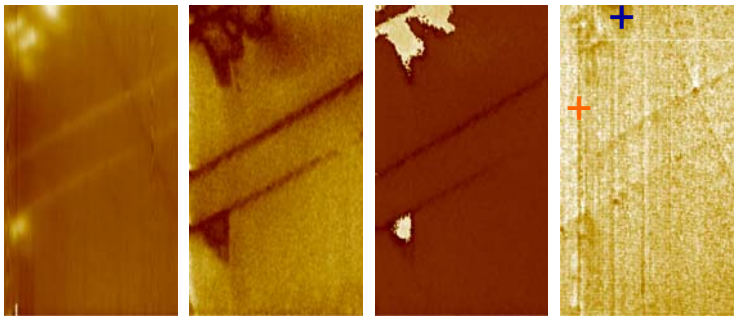

500 nm

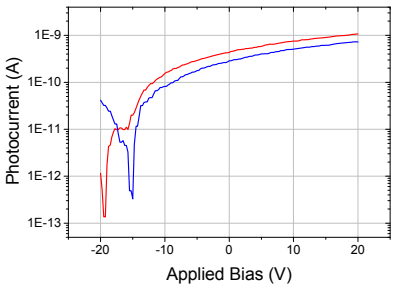

V_{OC}=-15 V

V_{OC}=-19.5 V

Correlation with the bulk properties

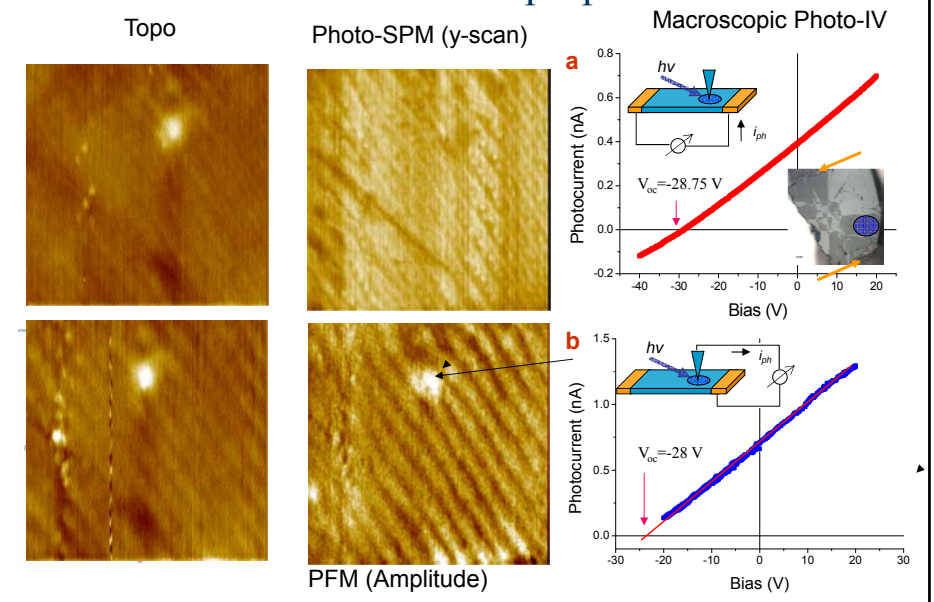

Photo-induced transient spectroscopy*

Nanoscale mapping of generation and recombination lifetimes

*M. Alexe, Nano Letters 12, 2193 (2012)

Photo-induced transient spectroscopy – PITS

Determination of deep levels in Cu-doped GaP using transient-current spectroscopy

Bruce W. Wessels

General Electric Corporate Research and Development, Schenectady, New York 12301
(Received 19 May 1975)

A method of determining deep levels in semiconductor junctions by observation of the temperature dependence of transient-current decay is described and applied to Cu-doped GaP. It is shown that the important deep-level parameters including trap energy, capture cross section, concentration, and recombination rate can be obtained. For Cu-doped GaP, several trapping levels were observed with energies of 0.50, 0.62, and 0.82 eV. Capture cross sections of these levels were of the order of 1×10^{-16} cm^2.

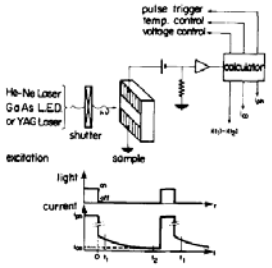

FIG. 1. Principle of the experiment.

Appl. Phys. Lett. 32(12), 15 June 1978

Laser 405 nm (3.08 eV)

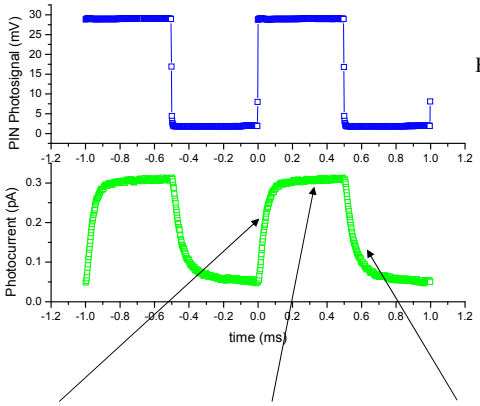

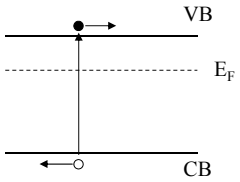

E_g=2.7 eV

Rate equation: $\frac{\partial n(t)}{\partial t} = G - R = G - \frac{n(t)}{\tau_{eff}}$

G - rate of excitation
R – recombination rate
n - photoinduced carrier density
τ - carrier (effective) lifetime

Rise curve: $n(t) = G\tau\left[1 - \exp\left(\frac{t}{\tau}\right)\right]$

Steady state $n(t) = G\tau$

Decay curve: $n(t) = G\tau \exp\left(-\frac{t}{\tau}\right)$

PITS-SPM

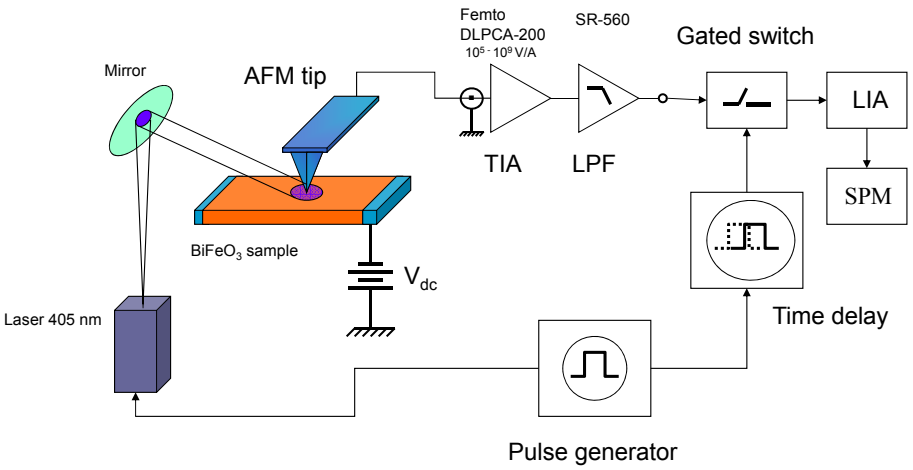

PITS-SPM

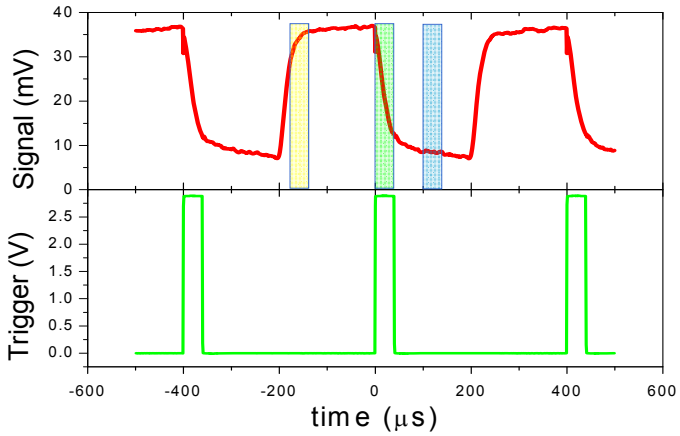

Generation

$$n(t) = G\tau\left[1-\exp\left(\frac{t}{\tau}\right)\right]$$

Recombination 1

$$n_1(t) = G\tau_1 \exp\left(-\frac{t}{\tau_1}\right)$$

Recombination 2

$$n_2(t) = G\tau_2 \exp\left(-\frac{t}{\tau_2}\right)$$

PITS-SPM on CdS single crystal

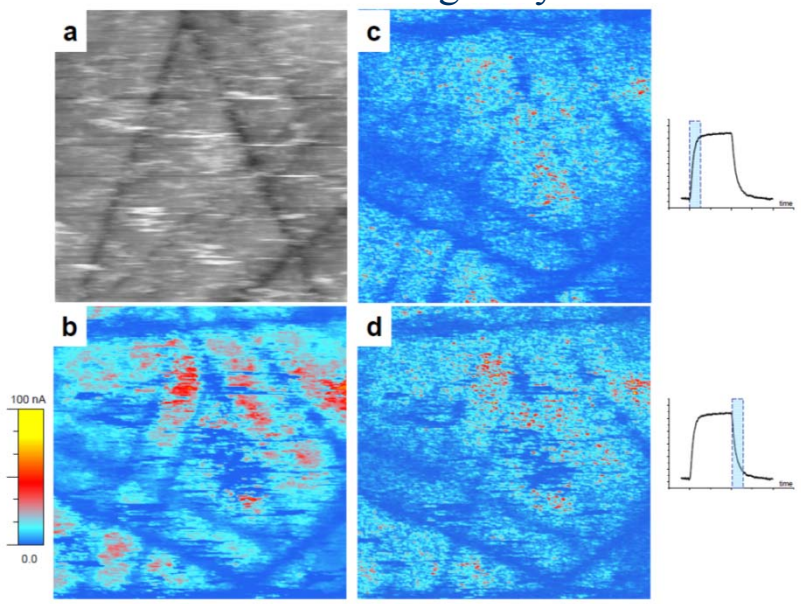

dc – photoconductive imaging

PITS-SPM on CdS single crystal

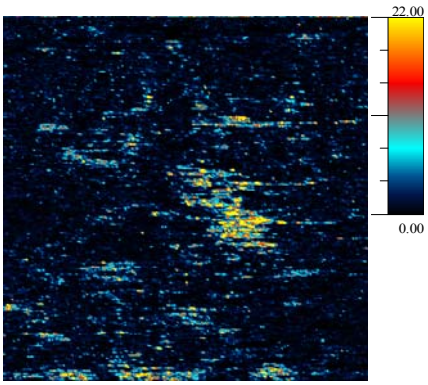

normalized PITS signals.

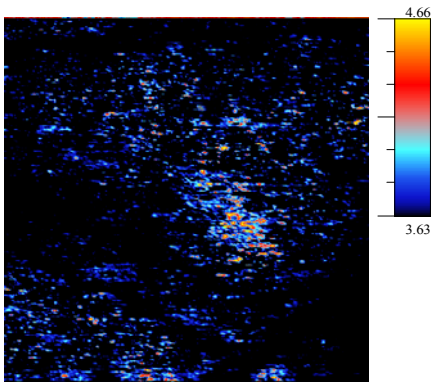

subtracted PITS signals.

Conclusion

- PITS-SPM is a powerful technique to map the defects and recombination centers
- Lateral resolution in the range of tip-surface contact diameter (20 nm)
- Temperature dependence will add energy resolution